A MEMS Vibrating Edge Supported Plate for the Simultaneous Measurement of Density and Viscosity: Results for Argon, Nitrogen, and Methane at Temperatures from (297 to 373) K and Pressures between (1 and 62) MPa†

Anthony R. H. Goodwin*

Schlumberger Doll Research, 36 Old Quarry Road, Ridgefield, Connecticut 06877

An edge supported plate fabricated by the methods of MicroElectroMechanical Systems (MEMS) is described that differs from the device reported by Goodwin et al. (*J. Chem. Eng. Data* **2006**, *51*, 190−208) in both design and plate area, which is about 2.4 times greater in this case. Two decoupled semiempirical equations are used, one for density and the other for viscosity, as reported by Goodwin et al. (*J. Chem. Eng. Data* **2006**, *51*, 190−208). Measurements were performed when a MEMS was immersed in argon, nitrogen, and methane at $T \approx 296$ K and pressures between (1 and 8) MPa and when another similar MEMS was immersed in argon and nitrogen at temperatures between (333 and 393) K and pressures in the range (20 to 62) MPa where the fluid viscosities are known to vary from (11 to 50) μPa·s and the densities cover the range (11 to 672) kg·m^{-3}. The unknown parameters in the semiempirical working equations were determined by calibration with argon. For the device exposed to pressures between (1 and 8) MPa for argon, nitrogen, and methane, the empirical expressions provided estimates of density within ± 0.5 % and viscosity typically within ± 1 % of the literature values, while the other device used for measurements with argon and nitrogen at pressures between (20 and 62) MPa at temperatures in the range (333 to 393) K gave densities that differed < ± 1 % and viscosities within ± 15 % of literature values.

Introduction

In a previous article,[1] an edge supported vibrating plate was described for the measurement of density and viscosity. The transducer was fabricated by the methods of MicroElectroMechanical Systems (MEMS). The measured complex resonance frequency was combined with a semiempirical model to determine density and viscosity. The model was validated in refs 1 and 2 by exposing the MEMS to methylbenzene and octane with densities between (619 and 890) kg·m^{-3} and viscosities in the range of (0.205 to 0.711) mPa·s and in ref 3 by immersion in argon at densities between (79 and 767) kg·m^{-3} and viscosities in the range (26 to 57) μPa·s. In refs 1 and 3, the coefficients of the working equations were determined with methylbenzene and argon, respectively. In ref 4, measurements were reported for fluids with viscosity between (0.038 and 275) mPa·s and densities in the range (408 to 1834) kg·m^{-3} at temperatures between (313 and 373) K and used to evaluate models and to propose a further working equation for the determination of density from the measured resonance frequency. Harrison et al.[5] have also reported measurements with the same design edge clamped plate MEMS immersed in fluids with viscosities between (0.4 and 100) mPa·s at densities in the range (600 to 1500) kg·m^{-3} and introduced an alternative working equation to that of ref 4.

In this article, an edge clamped plate of slightly different design and of both area and mass about 2.4 times greater than that of the devices reported in refs 1 to 4 and 5 was used to measure the density and viscosity of argon, methane, and nitrogen at densities in the range (11 to 672) kg·m^{-3} with viscosity between (11 and 50) μPa·s. Two similar devices were used, one for $T \approx 297$ K and pressures between (1 and 8) MPa and the other for temperatures between (333 and 393) K at pressures in the range (20 to 62) MPa.

Working Equations

Semiempirical working equations and analyses have been described in ref 1 with the density determined from eq 26 of ref 1 and the viscosity from eq 28 also of ref 1. Young's modulus, Poisson's ratio, and the density of the plate were also taken from ref 1. The working equations contain constants, C_i, with $i = 1$, 2, and 3, of proportionality determined by calibration. Over the range of conditions and substances studied, the fluid viscosity varied by a factor of about 5 and negated the requirement to utilize one or the other of the modified semiempirical expressions for density discussed in either ref 4 or 5. Details of the analysis procedures adopted have been described in ref 1 previously.

The plate used in this work was separated from the nearest object by more than 1 mm for all surfaces except the plate edges, which were about 0.25 mm from the 0.37 mm thick silicon surround. Other workers[6−10] have considered the vibration of a plate immersed in fluid as a function of separation from a stationary solid object. The results reported in refs 9 and 10 suggest the resonance frequency is affected when the oscillator of dimensions about 1 mm is separated from the solid object by less than 1 mm. These results are consistent with both our preliminary measurements[11] and the calculations of Green and Sader.[12] In our case, the ratio of the thickness of the plate to the separation is about 10.

* Corresponding author. Present address: Schlumberger, 125 Industrial Blvd., Sugar Land, TX 77478. Tel.: +1 281 285 4962. Fax: +1 281 285 8071. E-mail: agoodwin@slb.com.

† Part of the special issue "Robin H. Stokes Festschrift".

10.1021/je800491z CCC: $40.75
Published on Web 09/30/2008

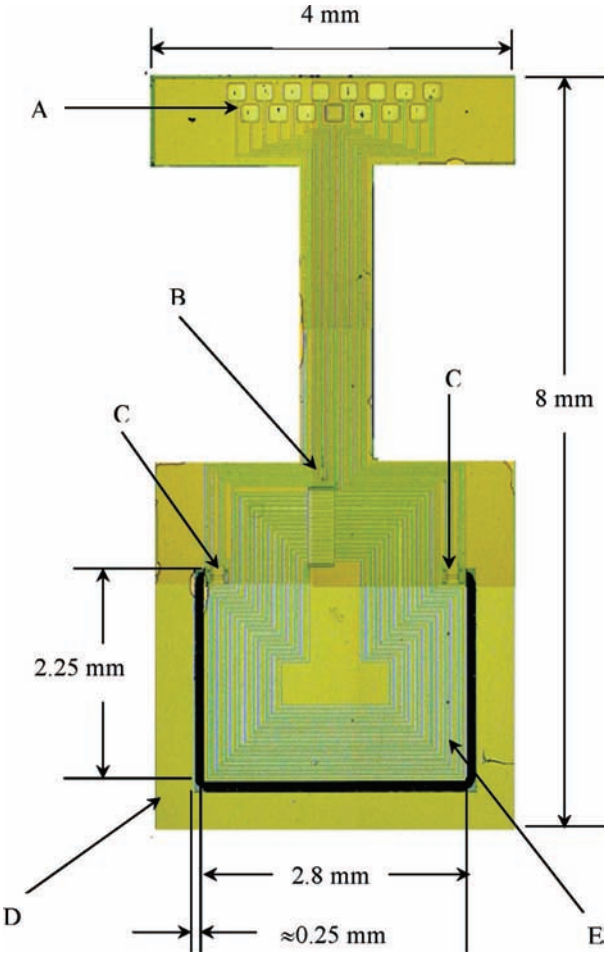

Figure 1. Photograph of the top surface of the MEMS showing the wire-bond pads A, thermometer B, Wheatstone bridges C, ≈370 μm silicon support D, and ≈22.25 μm thick plate E with coil of 16 turns of aluminum wire through which an alternating current is passed at a frequency close to the first eigenmode of the plate.

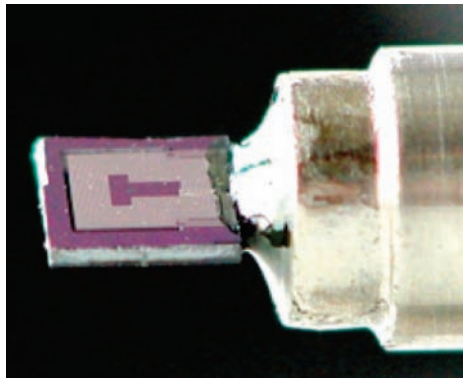

Figure 2. Photograph of the MEMS and the ≈6 mm o.d. stainless steel tube. Left: MEMS edge clamped vibrating plate with aluminum wire atop. Center: Adhesive. Right: type 316 stainless steel tube of outer diameter 6.35 mm.

Apparatus and Experimental Procedures

The design of the MEMS, shown in Figure 1, was similar to that of ref 1 and both are based on a device reported by Donzier et al.[13] The MEMS was fabricated at École Supérieure d'Ingénieurs en Électrotechnique et Électronique (ESIEE) with methods that are similar to those described by Bourouina et al.[14] The complete fabrication process has been described elsewhere,[1] and only the essential features are provided here.

Table 1. Resonance Frequency f, Resonance Line Half-Width g, and Quality Factor Q (= f/(2g)) for MEMS Device n at a Pressure of about $5 \cdot 10^{-3}$ Pa Determined with an Ionization Gauge Separated from the MEMS by about a 1 m Length of an 0.8 mm i.d. Tube[a]

n	T/K	$f(p \rightarrow 0)$/Hz	$g(p \rightarrow 0)$/Hz	Q
1[b,c]	296.301 ± 0.003	5088.3301 ± 0.0077	1.0001 ± 0.0077	2543.8
1[d]	296.805 ± 0.003	5086.751 ± 0.019	0.741 ± 0.019	3434.0
2[b]	333.160 ± 0.003	5352.6408 ± 0.0059	1.7491 ± 0.0059	1530.1
2	333.164 ± 0.003	5352.3608 ± 0.0373	1.668 ± 0.037	1604.5
2	353.139 ± 0.003	5347.800 ± 0.010	2.455 ± 0.010	1089.4
2	373.125 ± 0.003	5340.7977 ± 0.0099	4.395 ± 0.018	607.6
2	393.126 ± 0.003	5336.352 ± 0.022	7.234 ± 0.022	368.8

[a] Uncertainties in f and g determined from the fit of the in-phase and quadrature voltages measured as a function of frequency are at $k = 1$. [b] Used to determine C_1 and C_2. [c] Mean of three measurements. [d] Mean of two measurements.

The MEMS was processed on a 101.6 mm diameter silicon-on-insulator wafer (SOI) with a crystallographic plane (1,0,0) that consists of a 20 μm thick monocrystalline silicon fusion-bonded to silicon oxide (about 0.5 μm thick) that isolates the upper layer from the ≈350 μm monocrystalline silicon wafer below. The processes include the use of photolithography (as used in integrated circuit fabrication) and deep reactive ion etching for the micromachining.[15] Photolithography uses ultraviolet (UV) sensitive material (photoresist) and masks that define shapes, and after this combination is exposed to UV, the resulting patterned surface is chemically etched to remove the unwanted materials deposited onto the wafer to form particular elements, for example, resistors. To actuate and sense the plate motion as well as interconnect with the external electronics, nine boron-doped polycrystalline silicon resistors and aluminum wire, shown in Figure 1, were deposited atop the 20 μm monocrystalline silicon. Eight resistors formed two strain gauges each configured as a Wheatstone bridge and, as shown in Figure 1, were located at the two corners where the 20 μm thick plate met the underlying wafer; the two Wheatstone bridges can be used to either amplify the signal or identify other eigenmodes. The ninth resistor (not used in this work) could be used as a temperature detector. The deposited aluminum underwent photolithography to form a wire and provided an excitation coil of 16 turns as well as electrical connections between the wire-bond pads and the bridges and thermometer resistor as well as the coil used to excite motion. The edge supported plate was formed by micromachining and is, as Figure 1 shows, about 2.25 mm long and 2.8 mm wide separated on the remaining three edges from the surrounding frame, formed from the wafer of thickness ≈0.37 mm, by a distance of ≈0.25 mm. This surround was intended to serve as a protective barrier, for example, to deflect particulates in flowing media. Over the surface area of the plate, the thickness was estimated to be ≈22.25 μm. The MEMS, of width 4 mm and length 8 mm, was mounted on a printed circuit board, and all but the active element was sealed within a tube of type 316 stainless steel of outer diameter 6.35 mm, as shown in Figure 2, using adhesive as described in ref 1. Two MEMS, taken from the same wafer, were used in this work, one for the pressure range (1 to 8) MPa designated MEMS 1 and the other for pressures between (20 and 62) MPa given acronym MEMS 2. The first eigenmode imparts inertia to the support (as does the mode of similar symmetry in a vibrating tube densimeter),[16] and consequently, the 1 mm wide silicon connecting the wire-bond pads to the plate must be submersed, as shown in Figure 2, in adhesive; if mode (0,2) was used, the neck could be used as vibration isolation between the MEMS and its environment.

Table 2. Resonance Frequency *f*, and Resonance Line Half-Width *g* for the (0,1) Eigenmode of the Edge-Clamped Plate MEMS 1 Immersed in Fluid *i* at Temperature *T* and Pressure *p* with the Density ρ and Viscosity η Estimated from the Complex Resonance Frequency[a]

i	<*T*/K>	*p*/MPa	*f*/Hz	*g*/Hz	ρ/kg·m^{-3}	η/μPa·s
Ar[b,c]	297.247 ± 0.003	4.258 ± 0.022	3180.669 ± 0.022	31.177 ± 0.022	70.56 ± 0.77	23.46 ± 0.54
		5.137 ± 0.023	2993.869 ± 0.016	29.660 ± 0.016	85.48 ± 0.78	23.73 ± 0.46
		6.353 ± 0.023	2780.631 ± 0.011	27.726 ± 0.011	106.31 ± 0.79	24.12 ± 0.40
		7.146 ± 0.023	2663.271 ± 0.006	26.585 ± 0.006	119.96 ± 0.80	24.38 ± 0.37
		7.919 ± 0.023	2561.691 ± 0.047	25.585 ± 0.047	133.33 ± 0.81	24.68 ± 0.39
Ar[d]	296.630 ± 0.003	2.177 ± 0.022	3803.289 ± 0.067	34.177 ± 0.067	35.72 ± 0.74	22.78 ± 0.97
		3.077 ± 0.022	3492.830 ± 0.055	33.103 ± 0.055	50.79 ± 0.75	23.02 ± 0.72
		4.207 ± 0.022	3191.334 ± 0.046	31.222 ± 0.046	69.82 ± 0.77	23.39 ± 0.56
		5.389 ± 0.023	2943.990 ± 0.042	29.184 ± 0.042	89.99 ± 0.78	23.73 ± 0.46
		6.239 ± 0.023	2796.609 ± 0.052	27.835 ± 0.052	104.64 ± 0.79	24.00 ± 0.44
Ar[d]	295.862 ± 0.003	1.297 ± 0.022	4196.923 ± 0.115	33.562 ± 0.115	21.22 ± 0.73	22.61 ± 1.60
		2.184 ± 0.022	3798.799 ± 0.146	34.179 ± 0.146	35.91 ± 0.74	22.80 ± 1.03
		3.150 ± 0.022	3469.729 ± 0.166	33.009 ± 0.166	52.06 ± 0.76	23.08 ± 0.83
		4.240 ± 0.022	3182.043 ± 0.179	31.189 ± 0.179	70.47 ± 0.77	23.46 ± 0.76
		5.258 ± 0.023	2967.227 ± 0.156	29.436 ± 0.156	87.85 ± 0.78	23.78 ± 0.68
CH_4	296.381 ± 0.003	2.088 ± 0.022	4441.789 ± 0.065	22.303 ± 0.065	14.08 ± 0.31	11.30 ± 0.52
		3.247 ± 0.022	4161.693 ± 0.067	24.113 ± 0.067	22.35 ± 0.33	11.33 ± 0.36
		4.200 ± 0.022	3961.298 ± 0.055	24.691 ± 0.055	29.38 ± 0.34	11.56 ± 0.30
		5.397 ± 0.023	3739.027 ± 0.046	24.780 ± 0.046	38.53 ± 0.36	11.80 ± 0.25
		6.553 ± 0.023	3550.257 ± 0.042	24.565 ± 0.042	47.69 ± 0.37	12.09 ± 0.22
		8.184 ± 0.023	3318.881 ± 0.052	24.037 ± 0.052	61.12 ± 0.39	12.44 ± 0.21
N_2[e]	296.412 ± 0.003	0.950 ± 0.022	4566.704 ± 0.014	26.247 ± 0.014	10.9 ± 0.50	17.70 ± 1.65
		2.091 ± 0.022	4113.342 ± 0.022	30.030 ± 0.022	23.9 ± 0.51	17.73 ± 0.77
		3.116 ± 0.022	3803.274 ± 0.025	30.288 ± 0.025	35.7 ± 0.51	17.90 ± 0.53
		4.018 ± 0.022	3581.495 ± 0.024	29.769 ± 0.024	46.1 ± 0.52	18.11 ± 0.43
		5.093 ± 0.023	3361.930 ± 0.025	28.804 ± 0.025	58.4 ± 0.52	18.35 ± 0.36
		6.166 ± 0.023	3179.126 ± 0.027	27.741 ± 0.027	70.7 ± 0.52	18.60 ± 0.31
		7.188 ± 0.023	3030.990 ± 0.027	26.748 ± 0.027	82.3 ± 0.53	18.85 ± 0.28

[a] The uncertainties were determined from the standard deviation of the mean of *N* observations and are at a confidence interval of 0.95. [b] Used for calibration. [c] Purity 0.999999. [d] Purity 0.99999. [e] Purity 0.99998.

The MEMS evaluation apparatus and experimental procedures have been described elsewhere.[1,3] The resonant quartz pressure transducer described in refs 1 and 3 with an uncertainty of δp/MPa = ± {1·10^{-4}·(*p*/MPa) + 0.022} was used for $p \geq 20$ MPa. For $p < 20$ MPa, the pressure measurement with this device gives rise to $\delta\rho/\rho > 0.2$ %,[3] and another resonant quartz transducer with a maximum operating pressure of 8.2 MPa was used. When this $p < 8$ MPa gauge was calibrated against an oil-lubricated dead-weight gauge, it was found to have an uncertainty of δp/MPa = ± {0.0001·(*p*/MPa) + 0.0007}, where the quantity 0.007 MPa is about 0.01 % of the full-scale pressure. This pressure gauge does not introduce a significant error in the measured density at a pressure of 1 MPa. Pressures greater than that within the gas storage cylinders or 0.1 MPa were generated with an ISCO model 100 DX positive displacement pump with an upper operating pressure of about 68 MPa.

The uncertainty in the determination of resonance frequency depends on the Q {$= f/(2g)$} of the resonance. In this work, Q varied between 50 and 100 and was sufficient to obtain the density and viscosity with uncertainties less than 1 % and 10 %, respectively.

Temperature of the bath fluid was stable to within ± 3 mK as determined with a long-stem platinum resistance thermometer calibrated on ITS-90.

The following measurement procedure was adopted for each fluid: (1) the apparatus was thermostatted at about 373 K; (2) the apparatus was evacuated, with a turbo-molecular pump, to a pressure (as indicated by an ionization gauge located near the pump) of less than $<10^{-2}$ Pa for at least 24 h; (3) the system was flushed with the fluid to be used next from the positive displacement pump; (4) the apparatus cooled to and thermostatted at the lowest temperature of the measurements; (5) step 2 repeated; (6) the apparatus filled with the fluid to be investigated; (7) the complex resonance frequency measured at constant temperature as a function of pressure; (8) an aliquot of the sample flushed through the apparatus; (9) steps 7 and 8 repeated at least three times until the relative difference in resonance frequency between flushes was $<10^{-4}$; and (10) the complex frequency measured at the required temperature.

Materials. Two samples of argon, both supplied by Praxair Inc., Danbury, CT, were used, one with a mole fraction purity stated by the supplier of greater than 0.999999 and the other 0.99999, known as research and ultrahigh purity, respectively. The methane was research grade with a cited mass fraction purity of > 0.99999 and was supplied by MathesonTriGas that also provided two sources of nitrogen of stated purity of 0.99998, which had been water pumped, and the other of stated purity 0.99999 that are commonly known as zero gas and ultrahigh purity, respectively.

No analyses of the chemical compositions have been performed, and we have assumed for the samples used that there were no variations in chemical composition from those provided by the supplier.

Calibration. The parameters C_1 and C_2 of eq 26 of ref 1 and C_3 of eq 28 of ref 1 listed in Table 4 were determined with argon for both MEMS 1 and MEMS 2 with the measurements designated in Table 2 and Table 3, respectively, along with the $f(p \rightarrow 0)$ and $g(p \rightarrow 0)$ of Table 2. The observed $df(p \rightarrow 0)/dT$ is consistent with the observations reported in ref 1. The second row at $T = 333$ K lists values obtained after excursion to $T =$ 393 K, and the two $f(p \rightarrow 0)$ at this temperature differ by 0.005 %, while the Q vary by 5 %. For MEMS 1, the C_1 and C_2 of Table 4 accommodated the research purity argon measurements at $T \approx 296$ K and pressures between (1 and 8) MPa with a standard deviation $s(\rho)$ of the fit of 1.8 kg·m^{-3} ($100 \cdot s(\rho)/<\rho> = \pm 0.04$ %), while for MEMS 2 and the research grade argon at $T = 333$ K and pressure between (20 and 62) MPa the standard deviation $s(\rho)$ of the fit was 2.5 kg·m^{-3} ($100 \cdot s(\rho)/<\rho> = \pm 0.5$ %). For viscosity, the coefficient C_3 was determined at the same conditions as were C_1 and C_2. For

Table 3. Resonance Frequency f and Resonance Line Half-Width g for the (0,1) Eigenmode of the Edge-Clamped Plate MEMS 2 Immersed in Fluid i at Temperature T and Pressure p with the Density ρ and Viscosity η Estimated from the Complex Resonance Frequency[a]

I	$<T/K>$	p/MPa	f/Hz	g/Hz	ρ/kg·m^{-3}	η/μPa·s
Ar[b,c]	333.161 ± 0.003	20.940 ± 0.024	2034.19 ± 0.26	16.07 ± 0.26	304.5 ± 1.9	29.6 ± 2.0
		20.934 ± 0.024	2034.26 ± 0.14	15.90 ± 0.14	304.4 ± 1.9	31.2 ± 1.2
		27.895 ± 0.025	1816.14 ± 0.22	13.99 ± 0.22	395.2 ± 2.5	34.5 ± 2.3
		34.807 ± 0.025	1669.99 ± 0.26	13.10 ± 0.26	475.6 ± 2.9	35.0 ± 2.9
		34.803 ± 0.025	1669.39 ± 0.27	13.19 ± 0.27	475.6 ± 2.9	44.9 ± 3.7
		41.631 ± 0.026	1576.44 ± 0.36	13.79 ± 0.36	545.4 ± 3.3	41.8 ± 4.5
		41.611 ± 0.026	1576.95 ± 0.32	13.31 ± 0.32	545.3 ± 3.3	49.7 ± 4.8
		48.555 ± 0.027	1500.61 ± 0.18	13.52 ± 0.18	607.5 ± 3.7	49.7 ± 2.7
		48.542 ± 0.027	1500.46 ± 0.39	13.52 ± 0.39	607.4 ± 3.7	52.6 ± 6.1
		55.572 ± 0.028	1439.94 ± 0.32	13.12 ± 0.32	662.7 ± 4.0	49.7 ± 5.0
Ar[c]	353.141 ± 0.003	20.913 ± 0.024	2096.06 ± 0.23	19.44 ± 0.23	282.6 ± 1.8	31.3 ± 1.5
		20.910 ± 0.024	2097.00 ± 0.34	16.97 ± 0.34	282.5 ± 1.8	32.9 ± 2.7
		27.869 ± 0.025	1877.08 ± 0.60	17.41 ± 0.60	367.1 ± 2.3	31.4 ± 4.3
		27.861 ± 0.025	1878.36 ± 0.44	14.67 ± 0.44	367.0 ± 2.3	35.4 ± 4.3
		34.824 ± 0.025	1726.57 ± 0.26	15.60 ± 0.26	443.5 ± 2.7	38.1 ± 2.6
		41.722 ± 0.026	1619.05 ± 0.48	14.40 ± 0.48	511.1 ± 3.1	45.5 ± 6.1
		48.628 ± 0.027	1541.06 ± 0.12	14.39 ± 0.12	571.2 ± 3.5	43.3 ± 1.6
		55.616 ± 0.028	1478.36 ± 0.11	13.10 ± 0.11	625.2 ± 3.8	47.4 ± 1.8
		62.390 ± 0.028	1429.13 ± 0.10	12.92 ± 0.10	671.9 ± 4.1	47.3 ± 1.7
Ar[c]	373.147 ± 0.003	21.134 ± 0.024	2158.433 ± 0.057	18.654 ± 0.073	266.9 ± 1.7	35.03 ± 0.77
		27.925 ± 0.025	1930.818 ± 0.073	16.197 ± 0.053	344.1 ± 2.2	35.53 ± 0.71
		34.819 ± 0.025	1777.402 ± 0.053	15.217 ± 0.052	415.7 ± 2.6	39.32 ± 0.80
		41.670 ± 0.026	1666.752 ± 0.052	14.313 ± 0.094	480.0 ± 2.9	41.6 ± 1.3
		48.622 ± 0.027	1582.452 ± 0.094	13.722 ± 0.048	538.7 ± 3.3	44.22 ± 0.90
		55.539 ± 0.028	1516.954 ± 0.048	13.275 ± 0.056	590.9 ± 3.6	46.65 ± 1.06
		62.362 ± 0.028	1465.890 ± 0.056	12.991 ± 0.099	637.4 ± 3.8	49.3 ± 1.7
Ar[c]	393.115 ± 0.003	21.243 ± 0.024	2199.43 ± 0.21	18.41 ± 0.21	252.2 ± 1.7	32.5 ± 1.6
		28.020 ± 0.025	1977.44 ± 0.58	16.36 ± 0.58	324.7 ± 2.1	34.1 ± 4.9
		28.015 ± 0.025	1977.98 ± 0.06	16.77 ± 0.06	324.7 ± 2.0	35.74 ± 0.74
		34.800 ± 0.025	1823.90 ± 0.06	15.84 ± 0.06	391.5 ± 2.4	39.79 ± 0.88
		41.728 ± 0.026	1708.65 ± 0.11	15.57 ± 0.11	453.8 ± 2.8	46.0 ± 1.5
		48.708 ± 0.027	1621.92 ± 0.10	14.30 ± 0.10	510.6 ± 3.1	44.9 ± 1.4
		55.602 ± 0.028	1554.41 ± 0.12	14.54 ± 0.12	561.3 ± 3.4	52.3 ± 1.9
		62.423 ± 0.028	1498.04 ± 0.20	12.45 ± 0.20	606.9 ± 3.7	42.6 ± 2.7
N_2[d]	333.108 ± 0.003	20.991 ± 0.052	2435.093 ± 0.052	19.362 ± 0.052	196.2 ± 1.4	27.65 ± 0.55
		27.745 ± 0.057	2218.137 ± 0.057	17.106 ± 0.057	247.4 ± 1.7	27.36 ± 0.57
		34.853 ± 0.048	2062.291 ± 0.048	16.104 ± 0.048	294.5 ± 1.9	29.36 ± 0.57
		41.754 ± 0.041	1953.479 ± 0.041	15.638 ± 0.041	334.1 ± 2.0	32.02 ± 0.59
		49.710 ± 0.039	1860.385 ± 0.039	15.288 ± 0.039	373.9 ± 2.3	34.95 ± 0.63
		59.545 ± 0.045	1774.967 ± 0.045	15.044 ± 0.045	415.7 ± 2.5	38.53 ± 0.74

[a] The uncertainties were determined from the standard deviation of the mean of N observations and are at a confidence interval of 0.95. [b] Used for calibration. [c] Purity 0.99999. [d] Purity 0.99999.

Table 4. Values of C_i, with i = 1, 2, and 3, of Equations 26 and 28 of Reference 1 Obtained from Measurements with MEMS Device N = 1 in Argon at a Temperature of 296 K at Pressures between (1 and 8) MPa, Listed in Table 2, and for MEMS Device N = 2 at T = 333.15 K at Pressures Between (20 and 62) MPa, Listed in Table 3, Along with the $f(n, T, p\rightarrow 0)$ of Table 1

N	C_1	C_2	C_3/kg^2·m^{-4}·s^{-5}
1	0.993 612 5	4.340 550·10^{-2}	1.386 320 024·10^{11}
2	1.133 480 5	5.504 052·10^{-2}	3.126 659 757·10^{11}

MEMS 1 $100 \cdot s(\eta)/<\eta> = \pm 0.15$ %, and for MEMS 2, $100 \cdot s(\eta)/<\eta> = \pm 7$ %. These differences are taken as measures of the anticipated uncertainty in the measurements of density and viscosity obtained with the MEMS.

Literature Density and Viscosity. The reference densities were obtained from empirical representations of the Helmholtz function reported by Tegeler et al.[17] for argon, Setzmann and Wagner[18] for methane, and Span et al.[19] for nitrogen. The viscosity of methane was estimated from the work of Quinones-Cisneros et al.[20] and of argon and nitrogen from the transport property correlation of Lemmon and Jacobsen.[21] All of these correlations were coded within the National Institute of Standards and Technology, Standard Reference Database 23, Version 7.1, commonly known by the acronym REFPROP[22] and for the purpose of this work assumed exact.

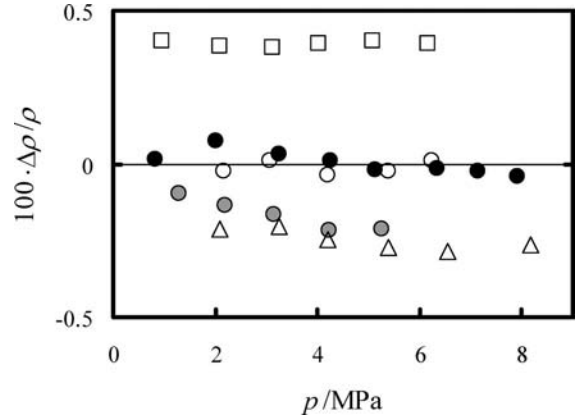

Figure 3. Fractional deviations $\Delta\rho/\rho = \{\rho(\text{expt}) - \rho(\text{lit})\}/\rho(\text{lit})$ of the experimental densities, ρ(expt), of Table 1 (obtained from eq 26 of ref 1 with the calibration coefficients C_1 and C_2 listed in Table 4) from the accepted values of refs 17, 18, and 19, ρ(lit), as a function of pressure p at $T \approx 297$ K. ●, argon $x > 0.999999$ (used to determine C_1 and C_2); ○, argon $x > 0.99999$; gray filled circle with black outline, argon $x > 0.99999$; □, water pumped nitrogen $x > 0.99998$; Δ, methane $x > 0.99999$.

Results and Discussion

The resonance frequency, f, and half the resonance line width, g, of the first eigenmode of the edge supported plate MEMS 1

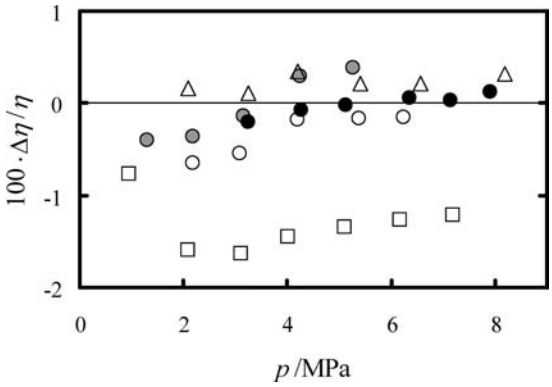

Figure 4. Fractional deviations $\Delta\eta/\eta = \{\eta(\text{expt}) - \eta(\text{lit})\}/\eta(\text{lit})$ of the experimental viscosity, η(expt), of Table 1 (obtained from eq 28 of ref 1 with the calibration coefficients C_3 listed in Table 4) from the accepted values of refs 20 and 21 η(lit), as a function of pressure p at $T \approx 297$ K. ●, argon $x > 0.999999$ (used to determine C_1 and C_2); ○, argon $x > 0.99999$; gray filled circle with black outline, argon $x > 0.99999$; □, water pumped nitrogen $x > 0.99998$; Δ, methane $x > 0.99999$.

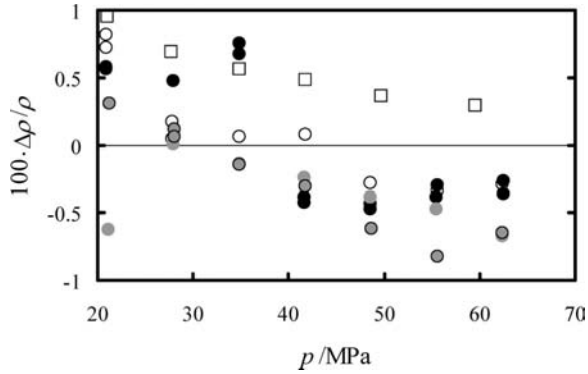

Figure 5. Fractional deviations $\Delta\rho/\rho = \{\rho(\text{expt}) - \rho(\text{lit})\}/\rho(\text{lit})$ of the experimental densities, ρ(expt), of Table 1 (obtained from eq 26 of ref 1 with the calibration coefficients C_1 and C_2 listed in Table 4) from the accepted values of refs 17, 18, and 19, ρ(lit), as a function of pressure, p. ●, argon $x > 0.999999$ at $T = 333$ K (used to determine C_1 and C_2); ○, argon $x > 0.999999$ $T = 353$ K; gray filled circle, argon $x > 0.999999$ $T = 373$ K; gray filled circle with black outline, argon $x > 0.999999$ $T = 393$ K; □, nitrogen $x > 0.999999$ $T = 333$ K.

immersed in argon, nitrogen, and methane at a temperature of 296 K at pressures between (1 and 8) MPa are listed in Table 2, while the f and g obtained with MEMS 2 in argon and nitrogen at temperatures between (333 and 393) K at pressures in the range (20 and 62) MPa are listed in Table 3. The density and viscosity, also listed in Table 2 for MEMS 1 and in Table 3 for MEMS 2, were obtained from eq 26 and eq 28 of ref 1, respectively, when combined with the C_1, C_2, and C_3 of Table 4. In the analysis, the temperature and pressure dependence of the plate dimensions and the density and elastic constants of silicon were included as described in ref 1. Small corrections have been applied to the viscosity and density reported in Table 2 and Table 3 to reduce all values to the stated temperature for each isotherm.

The combined expanded uncertainties, listed in Table 2 and Table 3, are for a coverage factor $k = 2$, that assuming a normal distribution represents a confidence interval of about 0.95, and were obtained by combining in-quadrature standard uncertainties arising from the transducer calibration with $(\partial\eta/\partial T)_p$ and $(\partial\eta/\partial p)_T$ for viscosity and $(\partial\rho/\partial T)p$ with $(\partial\rho/\partial p)_T$ for density. For the viscosity, the uncertainty in density obtained from the MEMS is also included.

The densities of argon, methane, and nitrogen obtained with MEMS 1 are shown in Figure 3 relative to the literature values

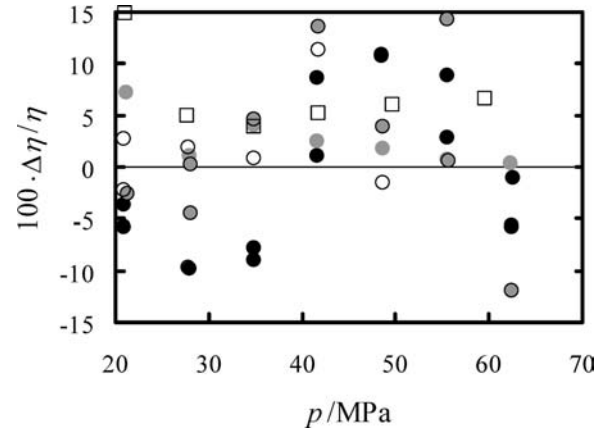

Figure 6. Fractional deviations $\Delta\eta/\eta = \{\eta(\text{expt}) - \eta(\text{lit})\}/\eta(\text{lit})$ of the experimental densities, η(expt), of Table 1 (obtained from eq 28 of ref 1 with the calibration coefficients C_1 and C_2 listed in Table 4) from the accepted values of ref 21, η(lit), as a function of pressure, p. ●, argon $x > 0.999999$ at $T = 333$ K (used to determine C_1 and C_2); ○, argon $x > 0.999999$ $T = 353$ K; gray filled circle, argon $x > 0.999999$ $T = 373$ K; gray filled circle with black outline, argon $x > 0.999999$ $T = 393$ K; □, nitrogen $x > 0.999999$ $T = 333$ K.

from refs 17, 18, and 19, respectively, and for argon, even from sources of different purity, and methane the results at pressures below 8 MPa lie within ± 0.3 %. However, the results for nitrogen show a constant systematic deviation with pressure of 0.4 %.

The values of viscosity obtained from MEMS 1 for argon, methane, and nitrogen are shown in Figure 4 as relative deviations from the correlations reported in refs 20 and 21. In this case, the viscosity obtained for argon, of all grades, and methane lies within ± 0.5 %, with one temperature-independent coefficient; however, the values obtained for nitrogen lie about 1.5 % below the literature values.

The relative deviations for nitrogen, while about 3 times lower than those reported in refs 1 and 3 for a different design MEMS, might arise from one or more of the following plausible sources: (1) the naivety of the assumption used to derive eq 26 of ref 1; (2) variations in the chemical composition; and (3) uncertainty in the literature values. In view of the source of the density from ref 19, item 3 is unreasonable and will not be considered further. Item 1 in light of the discussion in refs 4 and 5 will also not be considered further. No measurements were performed to negate item 2 as a source of error. However, the effect of variations in chemical composition on the measured density and viscosity of nitrogen can be estimated. Plausible impurities include hydrocarbons and for this gas sample water vapor. If we assume all of the observed density variations arise solely from water vapor, then a mole fraction of about 0.004 would be required; a value that is implausible but cannot be ruled out in the absence of measurements. The variation in viscosity is also consistent with the presence of water vapor with viscosity of about 10 μPa·s.[23]

At all densities obtained from MEMS 2 for argon and ultrahigh purity nitrogen in the temperature range from (333 to 393) K at pressures between (20 and 62) MPa, the relative deviations of our results from refs 17 and 19 fall, as shown in Figure 5, within ± 1 %. Such differences are as expected from work reported in ref 3. This agreement is remarkable given the simplicity of eq 26 of ref 1. The deviations, shown in Figure 5, have no significant temperature dependence and support the conjecture regarding the measurements shown in Figure 3 for water pumped nitrogen.

The values of viscosity obtained for nitrogen and argon from MEMS 2 are shown in Figure 6 as relative deviations from the correlation of Lemmon and Jacobsen,[21] and with one temperature-independent coefficient, all lie within ± 15 % consistent with the results obtained from the earlier design MEMS reported in ref 3.

To investigate the effect of varying viscosity on the measured density, preliminary measurements were performed with heptane obtained from Sigma-Aldrich with a mole fraction purity greater than 0.99. The resonance frequency and half-line-width of MEMS 2 were measured at a temperature of 333.1 K at pressures of (20.3, 40.0, and 40.8) MPa, and eqs 26 and 28 of ref 1 were used with the coefficients of Table 3, determined with argon, to obtain density and viscosity. The densities so determined were about 3 % above the correlation of Span and Wagner,[24] while the viscosity was 15 % below the estimate obtained from Assael et al.[25] These differences are similar to those reported in ref 1 for measurements with argon for a MEMS calibrated with methylbenzene and in ref 4.

Acknowledgment

The authors acknowledge Eric Donzier and Olivier Vancauwenberghe, both of Schlumberger-Doll Research, for their efforts with the design of the MEMS, Fredrick Marty and Bruno Mercier, both of ESIEE, for fabricating the MEMS, and Maria Manrique, of Schlumberger Cambridge Research, for packaging the MEMS.

Literature Cited

(1) Goodwin, A. R. H.; Donzier, E. P.; Vancauwenberghe, O.; Fitt, A. D.; Ronaldson, K. A.; Wakeham, W. A.; Manrique de Lara, M.; Marty, F.; Mercier, B. A Vibrating Edge Supported Plate, Fabricated by the Methods of Micro Electro Mechanical Systems for the Simultaneous Measurement of Density and Viscosity: Results for Methylbenzene and Octane at Temperature between (323 and 423) K and Pressures in the Range (0.1 to 68) MPa. *J. Chem. Eng. Data* **2006**, *51*, 190–208.

(2) Wakeham, W. A.; Fitt, A. D.; Ronaldson, K. A.; Goodwin, A. R. H. Measurement of Density and Viscosity with Vibrating Objects for Oilfield Applications Including Devices Fabricated by the Methods of MEMS. *High-Temp High-Press.*, accepted Jan. 2008.

(3) Goodwin, A. R. H.; Fitt, A.; Ronaldson, K.; Wakeham, W. A. A Vibrating Plate Fabricated with the Methods of Micro Electro Mechanical Systems (MEMS): Measurement of the Density and Viscosity of Argon at Temperatures Between 323 and 423 K at Pressures up to 68 MPa. *Int. J. Thermophys.* **2006**, *27*, 1650–1676.

(4) Goodwin, A. R. H.; Jakeways, C. V.; Manrique de Lara, M. A MEMS Vibrating Edge Supported Plate for the Simultaneous Measurement of Density and Viscosity: Results for Nitrogen, Methylbenzene, Water, 1-Propene,1,1,2,3,3,3-hexafluoro-oxidized-polymd and Poly-dimethylsiloxane, and Four Certified Reference Materials for Viscosity with Viscosities in the Range (0.038 to 275) mPa·s and Densities in the Range (408 to 1834) $kg \cdot m^{-3}$ at Temperatures between (313 and 373) K and Pressures up to 60 MPa. *J. Chem. Eng. Data* **2008**, *53*, 1436–1443.

(5) Harrison, C.; Ryu, S.; Goodwin, A.; Hsu, K.; Donzier, M. E.; Marty, F.; Mercier, B. A MEMS Sensor for the Measurement of Density-Viscosity for Oilfield Applications SPIE Photonics West 2006. In *Reliability, Packaging, Testing, and Characterization of MEMS/MOEMS V*; Tanner, D. M., Ramesham, R., Eds.; Proc. of SPIE, 2006, *6111*, 61110D.

(6) Clarke, R. J.; Cox, S. M.; Williams, P. M.; Jensen, O. E. The drag on a microcantilever oscillating near a wall. *J. Fluid Mech.* **2005**, *545*, 397–426.

(7) Clarke, R. J.; Jensen, O. E.; Billingham, J.; Williams, P. M. Three-dimensional flow due to a microcantilever oscillating near a wall: an unsteady slender-body analysis. *Proc. R. Soc. A* **2006**, *462*, 913–933.

(8) Clarke, R. J.; Jensen, O. E.; Billingham, J.; Pearson, A. P.; Williams, P. M. Stochastic Elastohydrodynamics of a Microcantilever Oscillating Near a Wall. *Phys. Rev. Lett.* **2006**, *96*, 050801.

(9) Chen, G. Y.; Warmack, R. J.; Huang, A.; Thundat, T. Harmonic response of near-contact scanning force microscopy. *J. Appl. Phys.* **1995**, *78*, 1465–1469.

(10) Naik, T.; Longnire, E. K.; Mantell, S. C. Dynamic Response of a cantilever in liquid near a solid wall. *Sens. Actuators, A* **2003**, *102*, 240–254.

(11) Harrison, C.; Tavernier, E.; Vancauwenberghe, O.; Donzier, E.; Hsu, K.; Goodwin, A. R. H.; Marty, F.; Mercier, B. On the response of a resonating plate in a liquid near a solid wall. *Sens. Actuators, A* **2007**, *134*, 414–426.

(12) Green, C. P.; Sader, J. E. Small amplitude oscillations of a thin beam immersed in a viscous fluid near a solid surface. *Phys. Fluids* **2005**, *17*, 073102−1 to 073102−12.

(13) Donzier, E.; Lefort, O.; Spirkovitvh, S.; Baillieu, F. Integrated Magnetic Field Sensor. *Sens. Actuators, A* **1991**, *25*−*27*, 357–361.

(14) Bourouina, T.; Spirkovitch, S.; Marty, F.; Baillieu, F.; Donzier, E. Silicon etching techniques and application to mechanical devices. *Appl. Surf. Sci.* **1993**, *65*−*66*, 536–542.

(15) Kovacs, G. T. A.; Maluf, N. L.; Petersen, K. E. Bulk Micromachining of Silicon. *Proc. IEEE* **1998**, *86*, 1536–1551.

(16) Chang, R. F.; Moldover, M. R. High-Temperature High-Pressure Oscillating Tube Densimeter. *Rev. Sci. Instrum.* **1996**, *67*, 251–256.

(17) Tegeler, Ch.; Span, R.; Wagner, W. A New Equation of State for Argon Covering the Fluid Region for Temperatures from the Melting Line to 700 K at Pressures up to 1000 MPa. *J. Phys. Chem. Ref. Data* **1999**, *28*, 779–850.

(18) Setzmann, U.; Wagner, W. A New Equation of State and Tables of Thermodynamic Properties for Methane Covering the Range from the Melting Line to 625 K at Pressures up to 1000 MPa. *J. Phys. Chem. Ref. Data* **1991**, *20*, 1061–1151.

(19) Span, R.; Lemmon, E. W.; Jacobsen, R. T.; Wagner, W.; Yokozeki, A. A Reference Quality Thermodynamic Property Formulation for Nitrogen. *J. Phys. Chem. Ref. Data* **2000**, *29*, 1361–1433.

(20) Quinones-Cisneros, S. E.; Huber, M. L.; Deiters, U. K. Reference Correlation for the Viscosity of Methane. *J. Phys. Chem. Ref. Data* **2008**, in preparation. Unpublished work reported in ref 19.

(21) Lemmon, E. W.; Jacobsen, R. T. Viscosity and Thermal Conductivity Equations for Nitrogen, Oxygen, Argon, and Air. *Int. J. Thermophys.* **2004**, *25*, 21–69.

(22) Lemmon, E. W.; McLinden, M. O.; Huber, M. L. *REFerence fluid PROPerties program 23*, version 7.1; Physical and Chemical Properties Division, National Institute of Standards and Technology: Boulder, Colorado.

(23) Kestin, J.; Sengers, J. V.; Kamgar-Parsi, B.; Levelt Sengers, J. M. H. Thermophysical Properties of Fluid H_2O. *J. Phys. Chem. Ref. Data* **1984**, *13*, 175–183.

(24) Span, R.; Wagner, W. Equations of State for Technical Applications. II. Results for Nonpolar Fluids. *Int. J. Thermophys.* **2003**, *24*, 41–109.

(25) Assael, M. J.; Dymond, J. H.; Papadaki, M.; Patterson, P. M. Correlation and Prediction of Dense Fluid Transport Coefficients. I. *n*-Alkanes. *Int. J. Thermophys.* **1992**, *13*, 269–281.

Received for review June 30, 2008. Accepted August 20, 2008.

JE800491Z